

Alma Mater Studiorum Università di Bologna  
Archivio istituzionale della ricerca

A cyber-physical system for clothes detection, manipulation and washing machine loading

This is the final peer-reviewed author's accepted manuscript (postprint) of the following publication:

*Published Version:*

Caporali A., Bedada W.B., Palli G. (2021). A cyber-physical system for clothes detection, manipulation and washing machine loading. Institute of Electrical and Electronics Engineers Inc. [10.1109/ICPS49255.2021.9468189].

*Availability:*

This version is available at: <https://hdl.handle.net/11585/832113> since: 2021-09-13

*Published:*

DOI: <http://doi.org/10.1109/ICPS49255.2021.9468189>

*Terms of use:*

Some rights reserved. The terms and conditions for the reuse of this version of the manuscript are specified in the publishing policy. For all terms of use and more information see the publisher's website.

This item was downloaded from IRIS Università di Bologna (<https://cris.unibo.it/>).  
When citing, please refer to the published version.

(Article begins on next page)

This is the final peer-reviewed accepted manuscript of:

A. Caporali, W. B. Bedada and G. Palli, "A Cyber-Physical System for Clothes Detection, Manipulation and Washing Machine Loading," *2021 4th IEEE International Conference on Industrial Cyber-Physical Systems (ICPS)*, 2021, pp. 519-524

The final published version is available online at [10.1109/ICPS49255.2021.9468189](https://doi.org/10.1109/ICPS49255.2021.9468189)

#### Rights / License:

The terms and conditions for the reuse of this version of the manuscript are specified in the publishing policy. For all terms of use and more information see the publisher's website.

***When citing, please refer to the published version of the article as indicated above.***

# A Cyber-Physical System for Clothes Detection, Manipulation and Washing Machine Loading

Alessio Caporali, Wendwosen Bellete Bedada, Gianluca Palli

**Abstract**—In this paper, a cyber-physical system for the detection and manipulation of clothes and its application to the problem of their robotized insertion in a washing machine drum is presented. Starting with the clothes randomly placed inside a bin next to the appliance, the method describes the approach used for the laundry bin picking together with a recovery picking from the drum door region in case some large cloth remains partially out from the washing machine. The same pointcloud-based perception algorithm is utilized for both tasks: the approaches are different only for what concerns the segmentation of the pointcloud for the extraction of the cloth-related points. The main algorithm exploits a wrinkledness measure to identify wrinkles in the cloth surface, to robustly assign spline curves to the detected wrinkle-like structure and to estimate grasping frames. In addition, a pointcloud registration technique is applied in the washing machine recovery task for the segmentation stage. The planning of the robot operations to execute the cloth grasping is also presented. The approach has been validated extensively by performing 100 trials grasps for both tasks.

**Index Terms**—Deformable Object Manipulation, Clothes State Estimation, Task-Priority Planning, Cyber-Physical Systems.

## I. INTRODUCTION

The sensing and manipulation of deformable objects (DOs) triggers diverse applications in various fields: from the medical domain with surgical assistance, passing by the industrial domain with food handling and end-of-line testing, but also domestic scenarios with household chores and clothing washing and ironing.

The challenge of manipulating and sensing DOs is massive due to their intrinsic property of being deformable. Indeed, their shape and appearance change during the time. This implies that the vast majority of the approaches and algorithm developed for rigid objects need to be modified or are not applicable at all to DOs.

Clothes are DOs characterized by having one dimension considerably smaller than the other two (i.e. the thickness of the fabric) [1]. Their sensing and manipulation have the same high number of possible industrial or domestic applications. Consider, as an example, the identification of clothes in an unstructured environment which is a fundamental requirement for assistive robots in domestic scenarios [2].

Alessio Caporali, Wendwosen Bellete Bedada and Gianluca Palli are with DEI - Department of Electrical, Electronic and Information Engineering, University of Bologna, Viale Risorgimento 2, 40136 Bologna, Italy.

This work was supported by the European Commission's Horizon 2020 Framework Programme with the project REMODEL - Robotic technologies for the manipulation of complex deformable linear objects - under grant agreement No 870133.

Corresponding author: [alessio.caporali2@unibo.it](mailto:alessio.caporali2@unibo.it)

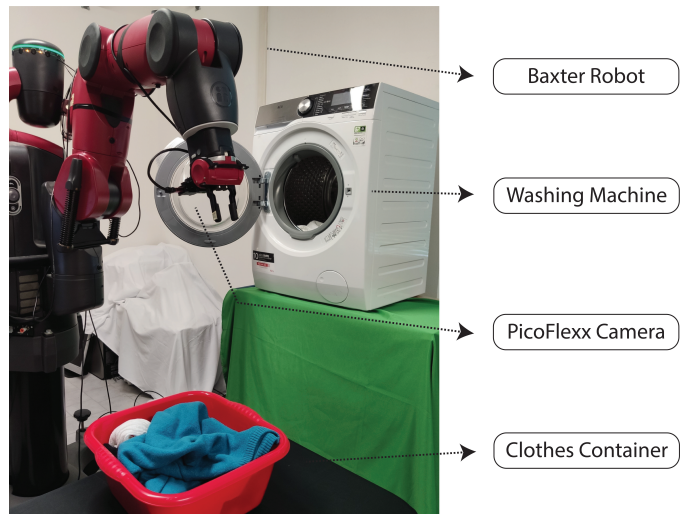


Fig. 1: Experimental setup.

In this paper, a cyber-physical system for the identification of grasping poses and the manipulation of clothes is presented addressing the picking of clothes from a container and from the drum door area of a washing machine. The first can be considered the primary task aiming at the robotized insertion of clothes, from a bin placed nearby, into a washing machine. The second, instead, can resemble a recovery strategy in case the insertion of a cloth was not completely achieved.

The core of the proposed approach is a pointcloud-based algorithm for the identification of optimal grasping poses in clothes having a crumpled configuration. The contribution of this paper is an extension and improvement of the algorithm originally proposed in [3]: the approach here presented preserves the same structure and main components while being able to selectively identify the wrinkles paths in a more robust and accurate way thanks to the interpolation of key points with spline curves. Secondly, in this paper, the initial segmentation step of the algorithm is also extended by addressing the problem of segmenting properly clothes hanging down from the washing machine door opening. The approach used is based on pointcloud registration. Finally, this paper focuses on the task-priority based planning of the robot activity to execute the grasps.

The experimental validation of the overall method is provided in this work by executing 100 grasp trials on a diverse clothes test sets for both tasks introduced.

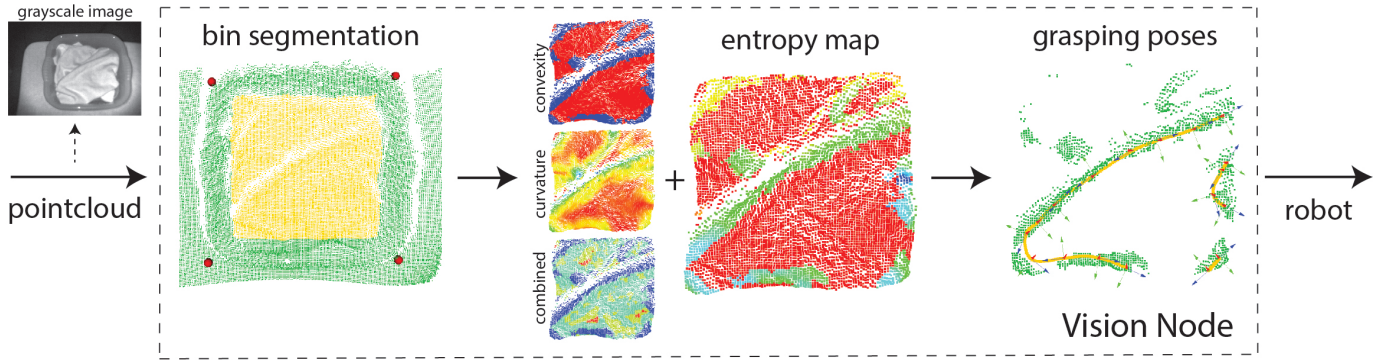


Fig. 2: Schema of the vision algorithm. The input pointcloud is segmented retrieving only the interior point of the bin (yellow). The entropy map is build utilizing the knowledge embedded into the convexity, curvature and combined (depth + edges) maps. The grayscale image is shown for clarity.

## II. LITERATURE REVIEW

A comprehensive review of the literature for sensing and manipulation of DOs is provided in a recent survey [1]. In this study, clothes are classified as biparametric objects not possessing any compression strength. The term biparametric indicates the object condition of having one dimension considerably smaller than its other two, i.e. the thickness of the fabric. Extensive work has emerged in the literature specifically related to cloth(es): state estimation of clothes [4]; grasp point detection [5] and [6]; manipulation tasks as grasping for garment picking-up [7] and [8], manipulation for garment reconfiguration [9] and [10]; manipulation for folding [11].

Clothes, due to the intrinsic nature, can assume infinite possible different shapes and, additionally, their color and texture can vary a lot as well. For this reasons, in the literature, wrinkles are emerged as key feature for working on textile objects.

Wrinkles can be used just for the identification of clothes in an unstructured environment, as in [12]. Here, the authors use a modified Gabor filter in conjunction with other techniques for extracting wrinkles features from an image and hence locate clothes in a domestic scene.

Additionally, wrinkles can carry important pieces of information for other tasks, as grasping, manipulation or flattening. In [13], a wrinkles analysis is carried out on a high definition 2.5D image. The principal dimensions of the wrinkles (height, width and volume) are estimated and used into a flattening strategy. In [5], wrinkles are identified via a graspability measure to decide the best candidate point for grasping the collar of clothes, the authors called it an informed grasp.

Specifically to the laundry operation, the location of the grasping point is not relevant. The only requirement is a stable grasp, since the clothes should be picked up from a container and placed inside the drum. In the literature, two different kind of approaches are present for selecting this type of grasping point: region based and wrinkle based.

In the region based approaches, the grasping point is chosen based on height information [14], centroid [9] or farthest

interior point to the border [15]. All this kind of methods present limits in case of non-convex areas [2].

Instead, an example of wrinkle based approach is the already mentioned work of [5]. Wrinkle based approaches represent a more robust alternative to the region based ones. Due to their shape, wrinkles are good candidate for grasping. In fact, the fingers of the gripper can be positioned at both sides of the ridge and an easy pinch grasp can follow [2].

## III. GRASPING POSE DETECTION

The grasping poses identification algorithm for cloth-like deformable objects has been already introduced in our previous work [3]. Here, we briefly recall the original approach and discuss the improvements and modifications introduced.

The algorithm consists of four distinct steps. The first performs the segmentation of the source pointcloud by identifying the bin in the scene and by broadcasting to the following steps only the points inside the bin itself. The second step applies a wrinkledness measure augmented by additional cues (convexity and depth) in order to find the areas of the segmented pointcloud with wrinkle-like structures. The third step is responsible for the fitting of a piecewise curve in each detected wrinkle area. The last step, number four, estimates a grasping pose for each piecewise wrinkle-path.

The improved version presented in this paper is based on the structure described but with major differences in the third (wrinkle-paths) and forth (poses estimation) steps. The first is described in Sec. III-A whereas the latter in Sec. III-B. Fig. 2 shows the flow of the discussed algorithm.

### A. Wrinkles as Interpolated Splines

The original piece-wise curve fitting presented in [3] turns out to be brittle and fragile, in particular for what concerns the nodes selection. To address these limitations, the new idea here exploited is to build an undirected graph  $G = (V, E)$  where the nodes ( $V$ ) are interconnected by the edges ( $E$ ) based on some properties. These nodes are arranged into a meaningful ordered sequence and a spline curve is interpolated to them.



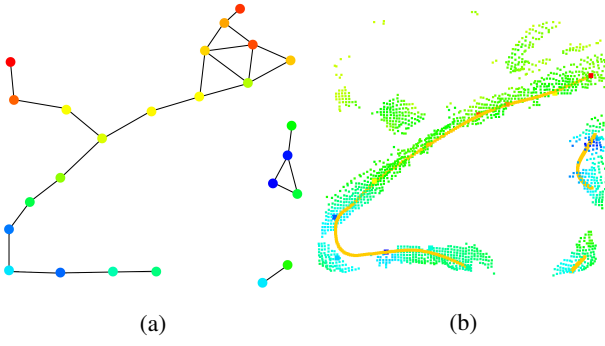


Fig. 3: Graph structure (a) and interpolated spline (b). In (a), the points in the graph denote the supervoxels centroids and the segments connecting them resemble the graph edges. The different colors in the nodes highlight their different intensities values. In (b), the segmented entropy map is shown in the background with the spline in yellow.

**Supervoxels Clustering:** The supervoxel clustering algorithm [16], utilized with the aim of creating the graph structure, is applied to the projected segmented entropy map (i.e. the output of step 2 in [3]).

The algorithm provides, for each supervoxel, its centroid points and the set of adjacent neighbours. The supervoxels centroids will be the nodes of the graph, the adjacency information is used for the introduction of edges. Each node is also augmented with an *intensity* attribute related to the wrinkledness score of the related area in the entropy map. Figure 3a displays the result of the clustering with the generated graph.

The obtained graph is clustered based on connected components resulting into a set of clusters (subsets)  $C_i$ ,  $i = 1, \dots, c$  where  $c$  is the number of clusters, such that  $G = \cup C_i$ .

**Path Building Process:** A path  $\mathcal{P}$  over a generic cluster  $C_i$  is a sequence of distinct alternating nodes and edges. We will denote the  $i$ -th path as  $\mathcal{P}_i = \{v_{i_1} \dots v_{i_l}\}$  where  $l$  is the total number of nodes denoting path  $i$ . From each cluster  $C_i$  a path is built by arranging the nodes of the graph into an ordered sequence. To build the path the following is performed: 1) selection of the maximum intensity node  $n_{\max}$ ; 2) recovery of the intensity values of its neighbours; 3) selection of the two neighbours with the largest intensities,  $n_{n1}$  and  $n_{n2}$ ; 4) building of two distinct temporary paths,  $\mathcal{P}_{\text{tmp}_1}$  and  $\mathcal{P}_{\text{tmp}_2}$ ; 5) merging into  $\mathcal{P}_i$  of the two paths.

Let's focus on  $\mathcal{P}_{\text{tmp}_1}$  only, since the process performed on  $\mathcal{P}_{\text{tmp}_2}$  is the same. The path building process is initialized by adding, in sequence,  $n_{\max}$  and  $n_{n1}$  to  $\mathcal{P}_{\text{tmp}_1}$  which was originally an empty queue. Given the path  $\mathcal{P}_{\text{tmp}_1}$  correctly initialized, the process loops inside an algorithm which aim is to propagate the path by adding as many node as possible.

Let's consider the last node of the path,  $n_l$ . Its neighbours  $N_l$  are checked and, among them, the remaining set of neighbours of  $n_l$  not in the path are processed and denoted *candidate nodes* with the symbol  $n_{c_i}$ , with  $i = 1 \dots s$ . The intensity and curvature scores for each candidate node  $n_{c_i}$  are evaluated. In particular, the product of wrinkledness score and

curvature score is performed. Then, the node with the greatest product score is selected as next node and added to the path. If all the candidate nodes have a product score of zero, then the path is assumed to have reached the end and hence the looping stopped.

Having computed both  $\mathcal{P}_{\text{tmp}_1}$  and  $\mathcal{P}_{\text{tmp}_2}$ , the final path  $\mathcal{P}_i$  is obtained just by merging the two portions using  $n_{\max}$  as junction point.

**Curvature Score:** The curvature score is evaluated between three nodes: the current last node of the path  $n_l$ ; the second last element  $n_{l-1}$ ; the candidate node  $n_{c_i}$ . So the angle between the two 3D vectors  $d_l = n_{l-1} - n_l$  and  $d_c = n_{c_i} - n_l$  can be computed and denote as  $\phi$ . The Von Mises distribution is used to transform the computed angle to a probability value. The Von Mises probability density function for the angle  $\phi$  is given by:

$$f(\phi \mid \mu, \kappa) = \frac{e^{\kappa \cos(\phi - \mu)}}{2\pi I_0(\kappa)} \quad (1)$$

where  $I_0(\kappa)$  is the modified Bessel function of order 0,  $\mu$  is the mean value ( $\mu = \pi$ ),  $\phi$  is the angle considered and  $\kappa$  is the measure of concentration ( $\kappa = 1$ ). With this setting we prioritize a smooth transition in the curvature between the nodes.

**Spline Interpolation:** The nodes centroids are translated from the projected space back to the original 3D space. Then, the nodes of each  $\mathcal{P}_i$  are fed as set of control points to be interpolated by a spline in the 3D space with a degree of 2. Notice that this is an approximated solution and different interpolation strategies can be implemented to refine it. The result of the interpolation for a sample pointcloud is denoted in Fig. 3b as a yellow curve.

## B. Poses Estimation

To enforce the estimation of an orthogonal axis with respect to the reference plane, the obtained spline curves are projected again to the reference plane.

On the projected splines, *target points* are extracted: each being the closest point on the spline curve to a given control node. The origin of a reference frame is assigned to each target point. The sliding axis of the frame is found by approximating the spline curve in that target point area with a tangent line. Due to the projection, the orthogonal axis comes for free as the third one. In the grasping poses of Fig. 2, the blue color indicates the sliding axes of the robot gripper (i.e. the wrinkle direction). We remark that, compared to having a single frame for spline curve [3], here we obtain  $n$  frames for each spline,  $n$  being the number of control nodes of the curve.

## IV. EXTENSION TO WASHING MACHINES

Inserting a cloth into the washing machine drum is a complex task. Due to many factors such as the initial point of grasp and topology/dimension of the cloth considered, it may happen that, after the insertion, a portion of the object lays outside the opening door of the washing machine drum. This situation would be problematic in case of a robotized washing

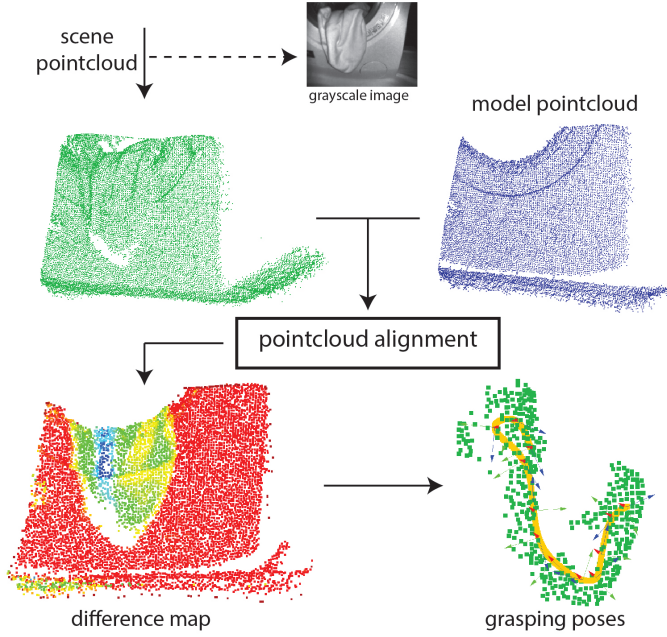


Fig. 4: Schema of the vision approach for the washing machine recovery picking. Grayscale image shown for clarity.

machine loading. A possible strategy for the identification and removal of clothes laying outside the drum door is here discussed by extending the approach presented in Sec. III about the bin segmentation.

The idea consists of using a pre-computed pointcloud model  $P_O$  of the washing machine for calculating a new pointcloud, named *difference map*  $P_D$ , as the difference between  $P_O$  and the current scene  $P_S$  pointclouds. The obtained  $P_D$  can be used for understanding if a misplaced cloth is present. Then, the grasping pose identification algorithm presented in Sec. III can be employed for computing the recovery poses for removing it. Fig. 4 provides a summary view of the approach described in this section.

#### A. Pointclouds Registration

In order to calculate  $P_D$ ,  $P_S$  and  $P_O$  should be aligned (i.e. registered). In particular, we need to find the transformation that would bring  $P_O$  to overlap  $P_S$ , obtaining the aligned model pointcloud  $P_{\hat{O}}$ . Notice that  $P_O$  is computed offline and represents a portion of a washing machine with the door opened. The alignment operation can be split into 1) the problem of determining the initial (rough) transformation between  $P_O$  and  $P_S$ , and 2) the optimization of the alignment.

The initial alignment is obtained by exploiting the Samples Consensus Prerejective (SCP) [17] method. It evaluates the correspondences between feature points, as features we select the Fast Point Features Histograms (FPFH) [18], and provides the initial guess for the transformation. This is refined by the Iterative Closest Point (ICP) algorithm [19] which minimize the Euclidean distance error metric between the overlapping areas of the pointclouds.

#### B. Difference Map

A reference plane is estimated from  $P_{\hat{O}}$  and both pointclouds are projected on this plane. Each point in  $P_S$  is matched with a point in  $P_{\hat{O}}$  and the two point-to-plane distances between each of them and  $p_{\text{ref}}$  are computed. Then the distances are evaluated and their difference stored inside  $P_D$ , Fig. 4 provides an example of *difference map* where the point intensity values are encoded in the color-map (reddish means close to zero). Thus,  $P_D$  is used to display the regions of the washing machine where  $P_{\hat{O}}$  and  $P_S$  differ the most.  $P_D$  is segmented by discarding all the points with a negligible difference (distance) based on an user-defined threshold. Notice that if all the points in the difference map do not satisfy the threshold, then this can be interpreted as a signal of not presence of misplaced cloth.

#### C. Grasping Poses Generation

The segmented  $P_D$  is employed directly from step 2 to the execution of the algorithm (Sec. III) aiming at finding possible recovery grasping poses (grasping poses example shown in Fig. 4). We remark that the only difference in the algorithm resides in the initial segmentation (step 1).

### V. TASK-PRIORITY BASED GRASP EXECUTION

A 7-DoFs robot arm is exploited for the implementation of the task under investigation. The arm is velocity controlled and, for grasp execution, the redundancy of the arm is exploited in the task-priority framework in such a way that low priority tasks are fulfilled in the null space of higher priority tasks [20]. The tasks implemented in the controller are, from the higher to lower priority, joint limit avoidance, end-effector pose control, elbow pose control, singularity avoidance and velocity minimizer task. For a general robotic system with n-DoF, in a given configuration,  $q = [q_1, q_2, \dots, q_n]^T$ , a forward kinematics of a particular task  $x \in \mathbb{R}^m$  can be expressed as a function of joint configuration:  $x(t) = x(q(t))$ . For such task variable, we also assume the existence of Jacobian relationship between task space velocity  $\dot{x}$  and the system velocity vector  $\dot{q}$  as  $\dot{x} = J(q)\dot{q}$ ; where  $J(q) \in \mathbb{R}^{m \times n}$  is the Jacobian matrix. Given a reference task space velocity vector  $\dot{\bar{x}}$ , the joint velocity vector  $\dot{q}$  that satisfies  $\dot{\bar{x}}$  in the least-square sense can be computed using the pseudoinverse as

$$\min_{\dot{q}} \|\dot{\bar{x}} - J\dot{q}\|^2 \implies \dot{q} = (J^T J)^\# J^T \dot{\bar{x}} \quad (2)$$

where the dependency of the Jacobian matrix from  $q$  is omitted for brevity and the symbol  $\#$  represents the matrix pseudoinverse. To manage multiple tasks that may be not all active at the same time, such as in case of tasks devoted to ensure joint limits or collision avoidance, the task activation matrix  $A$  is introduced into (2) to allow smooth transition during task activation and deactivation

$$\min_{\dot{q}} \|A(\dot{\bar{x}} - J\dot{q})\|^2 + \|J\dot{q}\|_{A(I-A)}^2 + \|V^T \dot{q}\|_P^2 \quad (3)$$

where  $V^T$  is the right orthonormal matrix of the SVD decomposition of  $J^T A J = U \Sigma V^T$  and  $P$  is a diagonal



Fig. 5: Grasp pose and generated way-points. From bin-top (a) and during washing machine recovery grasp (b).

regularization matrix where each element  $p_{(i,i)}$  is a bell-shaped function of the corresponding singular value of  $J$ , or zero if the corresponding singular value do not exist. The notation  $\|\cdot\|_P$  indicates the weighted norm, i.e.  $\|\dot{q}\|_P^2 = \dot{q}^T P \dot{q}$ . The generalized solution of (3) provides the desired arm joint velocity

$$\begin{aligned} \dot{q} = & (J^T A J + V^T P V)^\# J^T A A \dot{x} \\ & + (I - (J^T A J + V^T P V)^\# J^T A A J) \dot{q}_0 \end{aligned} \quad (4)$$

where  $\dot{q}_0$  can be exploited to implement lower priority tasks in hierarchy. Finally, the end-effector trajectory is generated in the operational space by interpolating the current pose and the grasp pose as shown in Fig. 5a and Fig. 5b, and the end-effector pose control task takes care of driving the robot along the desired path while ensuring the satisfaction of the other tasks according to their priority.

## VI. EXPERIMENTS

To validate the proposed approach, the algorithm is implemented in the ROS environment with the 7-DoF Baxter robot arm, while a 3D PicoFlexx camera in an eye-in-hand configuration is employed for the vision system. The schematic representation of the proposed cyber-physical system is reported in Fig. 6. In the experiments, the performance of the robot in the grasps with the poses provided by the proposed method is tested. Since the algorithm provides as output several target poses (one for each control node of the spline curves), we needed to decide which of the computed poses to use as reference for the experimentation. Concerning the bin picking task, we select as reference target pose the one with the greatest depth from the bin bottom plane. This to ensure a greater range of motion during the grasping operation. Regarding the task involving the washing machine, we prioritize the most distant pose from the drum center point, since this would allow the insertion of a greater portion of the cloth inside the drum.

Five clothes shown in Fig. 7 are used as test set. These clothes are selected in order to increase the variance for what concerns the dimensions of the item but also the type of fabric (e.g. "harder" or "softer") aiming at providing a comprehensive analysis. In this regard, the shirt has the softest fabric in the set, whereas the jeans have the hardest. The other clothes can be classified between them.

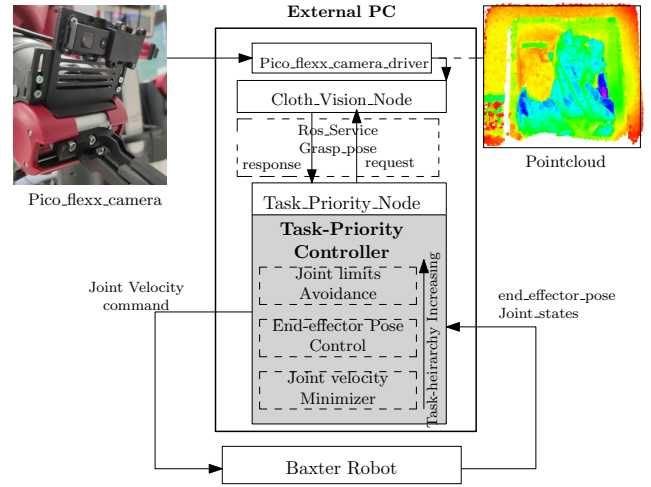


Fig. 6: Vision and control scheme implementation.



Fig. 7: Clothes test set with rulers in centimeters for scale.

### A. Grasability Tests

The experiments are carried out for the two tasks already introduced throughout this paper: the bin picking and washing machine recovery picking.

1) *Bin Picking Task*: This test is experimented having a single cloth of Fig. 7 in a bin. At the beginning of the experiment, the cloth is arranged into a random configuration. Then, the execution of the picking task is performed. In sequence, the vision system provides a new target pose (as explained in Sec. III), the robot attempt the grasp, lift the item 1 meter and release it. Hence, the cloth falls back down in the bin assuming a new random configuration. The picking task sequence is repeated 10 times for each cloth.

2) *Washing Machine Recovery Picking Task*: This test is carried out similarly to the bin picking one. The clothes of Fig. 7 are tested one at the time. For each cloth tested, 10 grasp trials are performed. The cloth is placed along the drum door partially hanging out from it to simulate an incorrect insertion. The vision system computes a target pose as described in Sec. IV. The robot attempts the grasp, moves the grasped cloth vertically toward the drum center, then it releases the grasp. In this case, after each grasp, the cloth is rearranged manually in a new configuration along the drum door.



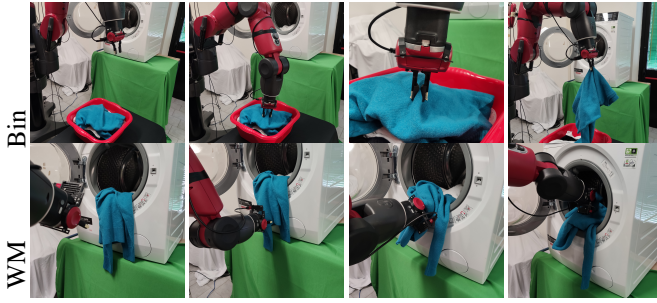


Fig. 8: Sequence of motion during laundry manipulation from Bin and Washing Machine (WM).

In Fig. 8 the sequence of actions performed for each task is depicted for clarity. Instead, Fig. 9 provides a chart showing the success rates of the grasps for the two tasks from the point of view of each type of cloth. The average success rate in the bin picking task is 0.70, while it is 0.82 in the washing machine one. Considering the total set of 100 grasps attempted, our algorithm provides a target pose that results on a successful grasp in 76% of the cases. The failure in the grasps are mostly related to wrong orientations of the target frame resulting from an erroneous identification of the wrinkle path. In a smaller extend, failures can be also associated to measurement errors of the camera, calibration errors for the eye-in-hand and accuracy of the robot arm itself.

#### B. Additional Experiment

A second type of experiments are performed related not only to the assertion of the correctness of the target poses provided by the algorithm, but also to the capability of those poses to allow the robot to reach a goal state with a reasonable amount of grasps. In particular, the capability of emptying a bin full of 4 test clothes is tested. Performing 5 trials, an average number of 5.2 grasps are required for accomplishing this tasks.

The capability of inserting completely a cloth hanging down from the drum door is also evaluated by performing 5 trials for each cloth tested. In this case, we adopt the small and big towels from the test set: for the first, an average number of 1.8 grasps are necessary; for the second, 3.2 grasps are needed;

It is important to remark that the trajectories used in those experiments are quite simple and the results are only preliminary since an in-depth study about the optimal trajectory and also grasp pose selection is still in progress.

### VII. CONCLUSIONS AND FUTURE WORK

In this paper, a pointcloud-based approach for the perception of clothes aiming at the robotized insertion of clothes inside a washing machine is proposed. The approach is validated extensively for both the bin picking and washing machine recovery picking tasks. The performances are satisfactory allowing a successful grasp in 76% of the attempts. In the future, we will work on integrating the approach presented into a complex robotic behavior fully autonomous. In addition, we will experiment about extending the approach to the picking of clothes from inside the washing machine drum.

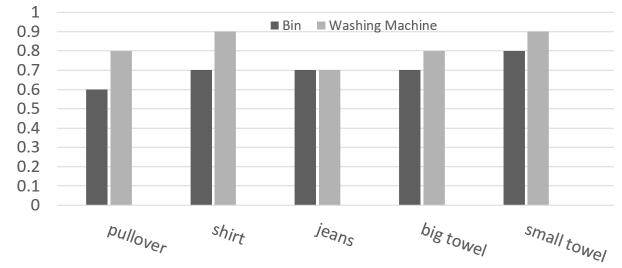


Fig. 9: Success rates for the bin picking and washing machine recovery picking actions.

### REFERENCES

- [1] J. Sanchez, J.-A. Corrales, B.-C. Bouzgarrou, and Y. Mezouar, "Robotic manipulation and sensing of deformable objects in domestic and industrial applications: a survey," *The Int. Journal of Robotics Research*, vol. 37, no. 7, pp. 688–716, 2018.
- [2] P. Jiménez and C. Torras, "Perception of cloth in assistive robotic manipulation tasks," *Natural Computing*, pp. 1–23, 2020.
- [3] A. Caporali and G. Palli, "Pointcloud-based identification of optimal grasping poses for cloth-like deformable objects," in *Proc. IEEE Int. Conf. on Factory Automation and Emerging Technologies*, 2020.
- [4] Y. Kita, F. Kanehiro, T. Ueshiba, and N. Kita, "Clothes handling based on recognition by strategic observation," in *Proc. IEEE ICRA*, 2011.
- [5] A. Ramisa, G. Alenya, F. Moreno-Noguer, and C. Torras, "Using depth and appearance features for informed robot grasping of highly wrinkled clothes," in *Proc. IEEE ICRA*, 2012.
- [6] K. Yamazaki, "Grasping point selection on an item of crumpled clothing based on relational shape description," in *Proc. IEEE/RSJ IROS*, 2014.
- [7] M. Shibata, T. Ota, and S. Hirai, "Wiping motion for deformable object handling," in *Proc. IEEE ICRA*, 2009.
- [8] P. Monsó, G. Alenya, and C. Torras, "Pomdp approach to robotized clothes separation," in *Proc. IEEE/RSJ IROS*, 2012.
- [9] M. Cusumano-Towner, A. Singh, S. Miller, J. F. O'Brien, and P. Abbeel, "Bringing clothing into desired configurations with limited perception," in *Proc. IEEE ICRA*, 2011.
- [10] A. Doumanoglou, A. Kargakos, T.-K. Kim, and S. Malassiotis, "Autonomous active recognition and unfolding of clothes using random decision forests and probabilistic planning," in *Proc. IEEE ICRA*, 2014.
- [11] J. Maitin-Shepard, M. Cusumano-Towner, J. Lei, and P. Abbeel, "Cloth grasp point detection based on multiple-view geometric cues with application to robotic towel folding," in *Proc. IEEE ICRA*, 2010.
- [12] K. Yamazaki and M. Inaba, "A cloth detection method based on image wrinkle feature for daily assistive robots," in *MVA*, 2009, pp. 366–369.
- [13] L. Sun, G. Aragon-Camarasa, S. Rogers, and J. P. Siebert, "Accurate garment surface analysis using an active stereo robot head with application to dual-arm flattening," in *Proc. IEEE ICRA*, 2015.
- [14] C. Bersch, B. Pitzer, and S. Kammel, "Bimanual robotic cloth manipulation for laundry folding," in *Proc. IEEE/RSJ IROS*, 2011.
- [15] B. Willimon, S. Birchfield, and I. Walker, "Classification of clothing using interactive perception," in *Proc. IEEE ICRA*, 2011.
- [16] J. Papon, A. Abramov, M. Schoeler, and F. Worgotter, "Voxel cloud connectivity segmentation-supervoxels for point clouds," in *Proc. IEEE Conf. on computer vision and pattern recognition*, 2013.
- [17] A. G. Buch, D. Kraft, J.-K. Kamarainen, H. G. Petersen, and N. Krüger, "Pose estimation using local structure-specific shape and appearance context," in *Proc. IEEE ICRA*, 2013.
- [18] R. B. Rusu, N. Blodow, and M. Beetz, "Fast point feature histograms (fpfh) for 3d registration," in *Proc. IEEE ICRA*, 2009.
- [19] R. B. Rusu, "Semantic 3d object maps for everyday manipulation in human living environments," *KI-Künstliche Intelligenz*, 2010.
- [20] W. B. Bedada, R. Kalawoun, I. Ahmadli, and G. Palli, "A safe and energy efficient robotic system for industrial automatic tests on domestic appliances: Problem statement and proof of concept," *Procedia Manufacturing*, vol. 51, pp. 454–461, 2020.